A Pilot Survey for Substructures in Class I Disks

None Assigned

ABSTRACT

We propose to search for and characterize substructures (gaps, spirals, clumps, etc.) in the spatial distributions of solid particles for 5 nearby Class I disks, using very high spatial resolution (~5 au scales) ALMA Band 6 continuum observations. This pilot survey will be among the first to resolve material well into the planet-forming zones of Class I disks with a uniform sensitivity and resolution (to a radius of ~2-3 au). In doing so, it will provide a homogenized look at the features that directly trace the planet formation process at an earlier stage than in the Class II disk Large Program we recently executed. We will quantify the prevalence, variety of form, spatial scales, spacings, symmetry, and amplitudes of disk substructures and connect those properties with theoretical ideas for their origins. This sample will fundamentally shape our understanding of how planet formation is aided by -- and perhaps reliant on -- disk substructures by constraining when such features form during the life cycle of circumstellar material. In doing so, it will provide essential context for the proper interpretation of disk observations at coarser resolutions.

PI NAME:	Sean Andrews			**SCIENCE CATEGORY:**	Circumstellar disks, exoplanets and the solar system
ESTIMATED 12M TIME:	**18.0 h**	**ESTIMATED ACA TIME:**	**0.0 h**	**ESTIMATED NON-STANDARD MODE TIME (12-M):**	**0.0 h**
CO-PI NAME(S): (Large & VLBI Proposals only)					
CO-INVESTIGATOR NAME(S):	Jane Huang; Myriam Benisty; Tilman Birnstiel; Xuening Bai; John Carpenter; Laura Perez; David Wilner; Andrea Isella; Karin Oberg; Viviana Guzman; Luca Ricci				
DUPLICATE OBSERVATION JUSTIFICATION:	N/A				

REPRESENTATIVE SCIENCE GOALS (UP TO FIRST 30)

SCIENCE GOAL	POSITION	BAND	ANG.RES.(")	LAS.(")	ACA?	NON-STANDARD MODE
IRAS 04016+2610 long baselines	ICRS 04:04:43.0710, 26:18:56.390	6	0.050 - 0.025	0.300	N	N
IRAS 04108+2803B long baselines	ICRS 04:13:54.7170, 28:11:32.900	6	0.050 - 0.025	0.300	N	N
IRAS 04166+2706 long baselines	ICRS 04:19:42.6270, 27:13:38.430	6	0.050 - 0.025	0.300	N	N
IRAS 04169+2702 long baselines	ICRS 04:19:58.4490, 27:09:57.070	6	0.050 - 0.025	0.300	N	N
IRAS 04295+2251 long baselines	ICRS 04:32:32.0550, 22:57:26.670	6	0.050 - 0.025	0.300	N	N
Short-Spacings Cluster	ICRS 04:04:43.0710, 26:18:56.390	6	0.300 - 0.150	1.700	N	N
Total # Science Goals : 6						

SCHEDULING TIME CONSTRAINTS	NONE	**TIME ESTIMATES OVERRIDDEN ?**	No

A Pilot Survey for Substructures in Class I Disks

1. Background and Motivation

Planet formation has historically been a theoretical venture: observational guidance has been primarily phenomenological, rather than quantitative, due to technological limits on angular resolution and sensitivity. That is quickly changing, as ALMA measurements of continuum emission from mm/cm-sized "tracer" particles in protoplanetary disks can now constrain how disk solids are spatially distributed at exquisite resolution (a few au for the nearest disks). ALMA has revealed azimuthal asymmetries (Casassus et al. 2013; van der Marel et al. 2013; Pérez et al. 2014), spiral patterns (Christiaens et al. 2014; Pérez et al. 2016), and concentric ring/gap morphologies (ALMA Partnership 2015; Andrews et al. 2016; Isella et al. 2016) in a serendipitous collection of disks. This past fall, we conducted an ALMA Large Program to study the forms, prevalence, and diversity of such substructures in the general disk population. While our analysis of these data is still in its preliminary stages (data delivery was only completed in mid-March), we do find that substructures are ubiquitous and exhibit a wide variety of scales, amplitudes, and morphologies: some representative examples are shown in Figure 1.

The evidence from ALMA strongly suggests that disk substructures are fundamental pieces of the planet formation puzzle. However, the interpretation of these features bifurcates into competing visions of their *origins*, and thereby their connections to the planet formation process. One branch considers an indirect link, postulating that the substructures trace particle "traps" where the migration of solids is stymied at local gas pressure maxima (Whipple 1972; Pinilla et al. 2012), induced by fluid instabilities (e.g., Bai & Stone 2014; Dipierro et al. 2015; Dullemond & Penzlin 2018) or steep gradients in material properties (e.g., Flock et al. 2015; Lyra et al. 2015; Okuzumi et al. 2016; Armitage et al. 2016). This perspective associates substructures with mechanisms that throttle solid migration rates and thereby strongly enhance the local solids-to-gas ratio. In that sense, the substructures are seen as essential environments for producing the planetesimal building blocks of terrestrial planets and giant planet cores (cf., Youdin & Shu 2002; Youdin & Goodman 2005; Johansen et al. 2009). The other interpretative branch draws a different conclusion: the substructures are instead a direct consequence of dynamical interactions between the disk material and *already-formed* planets. Such interactions can generate rings and gaps (e.g., Zhu et al. 2012; Dong et al. 2017; Bae et al. 2017), spirals (Zhu et al. 2015; Fung & Dong 2015; Bae & Zhu 2017), and asymmetries (e.g., vortices; Klahr & Henning 1997; Zhu & Stone 2014) if the formation of ∼super-Earths up to giant planets occurs very early in the disk's evolution, likely before the larger-scale envelope reservoir is dissipated (e.g., Nixon et al. 2018).

We aim to help develop a more comprehensive interpretation of the origins of these substructures and their roles in the planet formation process by probing their prevalence and forms *earlier* in the disk evolution sequence. The Class I disk population has a characteristic age of ∼0.5 Myr, much younger than the ∼2 Myr that is representative of the Class II disks that ALMA studies most frequently (Evans et al. 2009). A few recent results show that similar substructures are present in Class I disks (e.g., Sheehan & Eisner 2017b, 2018; see also ALMA Partnership et al. 2015), suggesting that crucial aspects of planet formation are well underway much earlier than we normally assume.

2. Immediate Objectives

We propose a pilot study to characterize substructures in the spatial distributions of solid particles for a sample of 5 nearby Class I disks, using high spatial resolution (∼5 au) Band 6 continuum observations. This program is designed to mimic the ALMA Large Program of Class II disks we have recently conducted, and thereby can serve as a complementary sub-sample that probes the properties of sub-

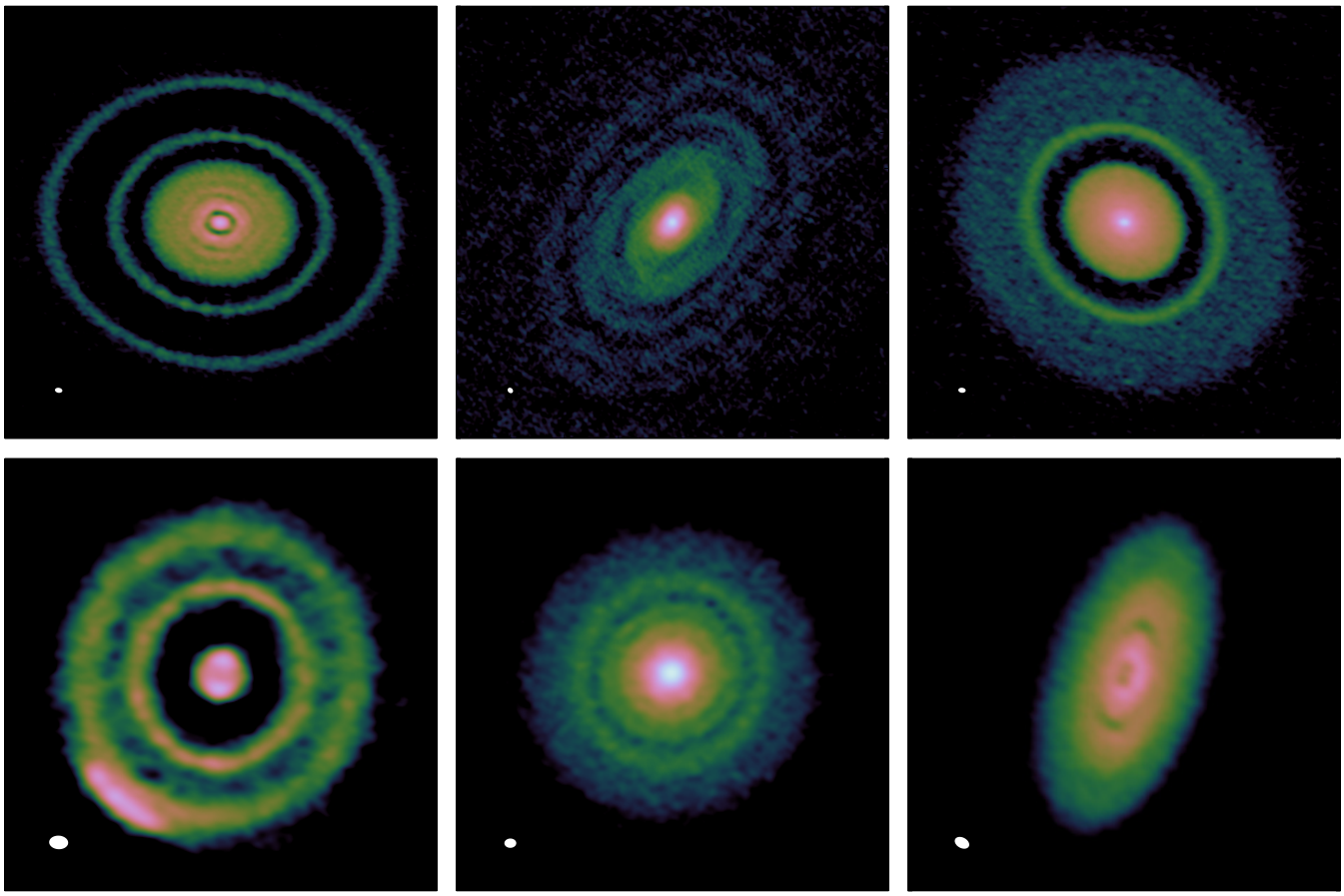

Figure 1: Some representative images of Class II disk substructures from the Cycle 4 Large Program we recently conducted (2016.1.00484.L; PI Andrews), showing a range of feature scales and amplitudes, as well as morphological diversity. The beam sizes are in the lower left corner of each panel, and give a sense of scale (each is ∼5 au in diameter); note the panel extents are different. These disk targets have comparable inner disk brightnesses as the Class I disks being selected here, and the observational strategy is essentially identical: the expectation is that the proposed data will be of similar quality.

structures along the evolutionary dimension. In either perspective for the origins of these substructures, there is great interest in identifying when they form and whether their general characteristics evolve with time. For example, MHD models predict that magnetic field strength decreases as disks evolve (Bai & Stone 2017). The Class 0/I phases should be more strongly magnetized, which drives more vigorous accretion. This state could riddle the Class I disks with rings and gaps due to the anisotropic nature of ambipolar diffusion (Bethune et al. 2017; Suriano et al. 2018). In this scenario, ring/gap substructures should be prevalent in Class I systems, and Class II disks might simply inherit such substructures. Or alternatively, if planet formation begins early, as some have inferred based on the small fraction of massive Class II disks in demographic surveys (Najita & Kenyon 2014; Ansdell et al. 2016) compared to their Class I counterparts (Sheehan & Eisner 2017a), we expect to see a diversity of structures including ring/gaps, vortices, and/or spirals even during the Class I phase that would set important constraints on the relevant initial conditions and timescales. In any case, the proposed observations will be among the first to resolve material well into the planet-forming zones (to $r \sim 2$–3 au) of Class I disks with a uniform sensitivity and resolution. In doing so, they will provide a homogenized look at the features that help trace the planet formation process at very early times, quantifying their prevalence, variety of form, spatial scales, spacings, symmetry, and amplitudes.

To construct a sample, we considered the Taurus-Auriga association ($d \approx 140$ pc) because it currently has the best-characterized Class I population and is well-suited to nighttime long-baseline observations during Cycle 6 (C43-8/9). There are ∼20 Class I sources in this region.[1] Seven of those have not yet been observed with an interferometer: we exclude those targets because we cannot reliably associate emission with a disk rather than an envelope, and therefore cannot estimate a required sensitivity at high resolution. Five other targets have already been observed with ALMA at sufficiently high resolution, although the results from only one of these have been published at the time of writing (HL Tau; ALMA Partnership et al. 2015). Of those, 2 are relatively evolved (i.e., borderline Class II), and 2 others have edge-on viewing geometries that could artificially obscure substructures (due to high optical depths and/or projection effects). This indicates that the Taurus Class I sources observed with ALMA so far are not ideal for assessing the prevalence of substructures. The 8 remaining Taurus Class I sources were observed with CARMA at 230 GHz with sub-arcsecond resolution (Eisner 2012; Sheehan & Eisner 2017a). We used those observations, and the associated modeling results that differentiate disk and envelope emission, to down-select following the same methodology as for the Class II ALMA Large Program. We conservatively assumed that the (as yet unresolved) emission in the disk centers (within a ∼60 au FWHM beam) is smooth (i.e., no substructure) and made simple power-law models of the brightness distribution at 5 au resolution. In that bound, the brightness distribution at all scales ≥5 au can be recovered in a reasonable observation for disks that emit ≥20 mJy from their inner regions ($r \leq 30$ AU). The target sensitivity is a $5\,\sigma$ limit of 85 μJy per 5 au beam (RMS = 17 μJy beam^{-1}). If substructures are present, they will be detected at even higher confidence (regardless of their optical depths). So, the primary selection criterion is a cut on *surface brightness* in the inner disk. Finally, we also employ the criterion that the reported target inclination (reported by Sheehan & Eisner 2017a) is low enough ($i < 65°$) to avoid projection/optical depth effects that could obscure substructures.

The resulting sample includes 5 Class I sources: IRAS 04016+2610 (= L1489 IRS), IRAS 04108+2803B, IRAS 04166+2706, IRAS 04169+2702, and IRAS 04295+2251. Combined with the other cases that will eventually have high (sub-10 au) resolution images in the ALMA archive, our sample will result in a census for substructures in half the Taurus Class I disk population and span a significant range in host luminosity and disk-to-envelope mass ratios (proxies for host mass and evolutionary state).

3. Strategy & Technical Feasibility

With the data we are proposing to obtain, we can expect to *resolve* gaps from giant planets (0.1–1 $M_{\rm Jup}$) in these disks at orbital radii down to ∼15–20 au; we should be able to detect (unresolved) gaps at orbital radii ≥5 au. The gas pressure scale height, h (where $h/r \sim 0.1$), is also a benchmark scale for turbulent substructures. We can *resolve* h-scale features in radius/azimuth at $r \geq$ 40–50 au, and should detect them down to $r \sim 10$ au. The proposed sensitivity enables firm detections of small-scale variations at the ∼2% (inner disk) to 10% (outer disk) level, enough to see the ∼20% contrasts expected for gaps opened by >0.1 $M_{\rm Jup}$ planets (Fung et al. 2014), zonal flows (Simon & Armitage 2014), and weak vortices (Goodman et al. 1987). Meeting these benchmarks for substructure at these physical scales is not possible at any coarser resolution or with more modest sensitivity (i.e., shorter integrations, even at high resolution, will miss the shallow contrasts we see frequently for substructures in the Class II disk population). The Class II disk Large Program verifies that substructures are present down to these scales and amplitudes at that evolutionary stage: we seek to find out if they are present, and if so similar, or perhaps more or less pronounced, at earlier times.

[1] There is some ambiguity in the infrared spectrum-based definition; e.g., whether or not one includes "flat-spectrum" sources as Class I or II. But 20 is roughly speaking the size of the full population.

One of the primary reasons we have not yet seen a large volume of ALMA results for Class I disks is the perception that the separation of inner envelope and disk emission remains a challenge (or, more accurately, is highly model dependent). That conservatism is reasonable; this is a challenging problem. However, in the very specific context of the program we are proposing, distinguishing between the "inner envelope" and the "disk" on radial scales of a few tens of au, and at resolutions of $\sim$5 au, is besides the point. The answers to the basic question we are asking – are there substructures with similar morphologies and scales at comparable locations to those seen in the Class II disk population? – are agnostic about which circumstellar component is associated with that material. Nevertheless, we appreciate that some information about the envelopes can be useful, particularly in terms of understanding the temperature structures in the system as inputs for future interpretative models (e.g., hydrodynamics simulations, or for scenarios that rely on the locations of volatile condensation fronts). To that end, we are including the CO J=2$-$1 main isotopologues in the accompanying short-spacings observations (C43-5/6), with the goal of helping to characterize the gas densities and kinematics on angular scales traditionally associated with the disk/envelope transition region in Class I sources. To be conservative, we will maximize the continuum bandwidth for the observations with the longest baselines: the Class II disk Large Program makes clear that the line emission from most disks at sub-0.1″ resolution requires a substantially larger time investment that is not yet justified for this sample.

Our philosophy for analyzing such data is to focus first on a quantitative, (data-driven) phenomenological characterization of the substructure as observed (i.e., in terms of the scales and amplitudes of surface brightness features, rather than physical conditions). Without knowing what we are facing at these resolution scales, it seems pre-mature to force a parametric model/simulation to fit the data. Once the basic analysis of the sample is underway, we will endeavor to interpret key features in the contexts of detailed models for planet-disk interactions, the evolution of disk solids, and global-scale magnetic structures, all grounded in radiative transfer simulations (using `RADMC-3D`), all of which we are developing now for interpreting data in the Class II disks ALMA Large Program. Ultimately, these observations and this template for analysis will serve as important guides for interpreting future observations of Class I disks in general and their substructures in particular.

References

ALMA Partnership et al. 2015, *ApJ*, 808, L3 • Andrews et al. 2016, *ApJ*, 820, L40 • Ansdell et al. 2016, *ApJ*, 828, 46 • Armitage et al. 2016, *ApJ*, 828, L2 • Bae et al. 2017, *ApJ*, 850, 201 • Bae & Zhu 2017, *ApJ*, in press (arXiv:1711.08161) • Bai 2017, *ApJ*, 845, 75 • Bai & Stone 2014, *ApJ*, 796, 31 • Bai & Stone 2017, *ApJ*, 836, 46 • Bethune et al. 2017, *A&A*, 600, 75 • Casassus et al. 2013, *Nature*, 493, 91 • Christiaens et al. 2014, *ApJ*, 785, L12 • Dipierro et al. 2015, *MNRAS*, 451, 974 • Dong et al. 2017, *ApJ*, 843, 147 • Dullemond & Penzlin 2018, *A&A*, 609, 50 • Eisner 2012, *ApJ*, 755, 23 • Evans et al. 2009, *ApJS*, 181, 231 • Flock et al. 2015, *A&A*, 574, 68 • Fung et al. 2014, *ApJ*, 782, 88 • Fung & Dong 2015, *ApJ*, 815, L21 • Goodman et al. 1987, *MNRAS*, 225, 695 • Isella et al. 2016, *PRL*, 117, 251101 • Johansen et al. 2009, *ApJ*, 697, 1269 • Klahr & Henning 1997, *Icarus*, 128, 213 • Lyra et al. 2015, *A&A*, 574, 10 • Najita & Kenyon 2014, *MNRAS*, 445, 3315 • Nixon et al. 2018, *MNRAS*, in press (arXiv:1803.14407) • Okuzumi et al. 2016, *ApJ*, 821, 82 • Pérez et al. 2014, *ApJ*, 783, L13 • Pérez et al. 2016, *Science*, 353, 1519 • Pinilla et al. 2012, *A&A*, 538, 114 • Sheehan & Eisner 2017a, *ApJ*, 851, 45 • Sheehan & Eisner 2017b, *ApJ*, 840, L12 • Sheehan & Eisner 2018, *ApJ*, in press (arXiv:1802.02847) • Simon & Armitage 2014, *ApJ*, 784, 15 • Suriano et al. 2018, *MNRAS*, in press (arXiv:1712.06217) • van der Marel et al. 2013, *Science*, 340, 1199 • Whipple 1972, *From Plasma to Planet*, 211 • Youdin & Shu 2002, *ApJ*, 580, 494 • Youdin & Goodman 2005, *ApJ*, 620, 459 • Zhu et al. 2012, *ApJ*, 755, 6 • Zhu & Stone 2014, *ApJ*, 795, 53 • Zhu et al. 2015, *ApJ*, 813, 88

None Assigned

SG : 1 of 6 IRAS 04016+2610 long baselines Band 6

C43-8/9 observations to 17 uJy/beam.

Science Goal Parameters

Ang.Res.	LAS	Requested RMS	RMS Bandwidth	Rep.Freq.	Cont. RMS	Cont. Bandwidth	Poln.Prod.	Non-standard mode
0.0500" - 0.0250"	0.3"	17 µJy, 151.2 mK-604.8 mK	9588.245 km/s, 7.5 GHz	234.500000 GHz	16.944 µJy, 150.7 mK-602.8 mK	7.500 GHz	XX,YY	No

Use of 12m Array (43 antennas)

t_total(all configs)	t_science(C43-8,C4...	t_total()	Imaged area	#12m pointing	12m Mosaic spacing	HPBW	t_per_point	Data Vol	Avg. Data Rate
3.2 h	1.3 h	0.0 h	8.3 "	1	offset	24.8 "	4717.2 s	25.2 GB	3.3 MB/s

Use of ACA 7m Array (10 antennas) and TP Array

t_total(ACA)	t_total(7m)	t_total(TP)	Imaged area	#7m pointing	7m Mosaic spacing	HPBW	t_per_point	Data Vol	Avg. Data Rate

Spectral Setup : Single Continuum

Center Freq (Sky)	Center Freqs. SPWs	Eff #Ch p.p.	Bandwidth	Resolution	Vel. Bandwidth	Vel. Resolution	RMS
225.500000	216.500000	128	1875.00 MHz	31.250 MHz	2596.4 km/s	43.273 km/s	30.84 µJy, 1.3 K
	218.500000	128	1875.00 MHz	31.250 MHz	2572.6 km/s	42.876 km/s	30.93 µJy, 1.3 K
	232.500000	128	1875.00 MHz	31.250 MHz	2417.7 km/s	40.295 km/s	32.74 µJy, 1.2 K
	234.500000	128	1875.00 MHz	31.250 MHz	2397.1 km/s	39.951 km/s	34 µJy, 1.2 K

1 Target

No.	Target	Ra,Dec (ICRS)	V,def,frame --OR--z
1	1-IRAS_04016+2...	04:04:43, 26:18:56	4.00 km/s,lsrk,RADIO

Expected Source Properties

	Peak Flux	SNR	Linewidth	RMS (over 1/3 linewidth)	linewidth / bandwidth used for sensitivity	Pol.	Pol. SNR
Line	0.00 uJy	0.0	0 km/s			0.0%	0.0
Continuum	3.00 mJy	177.1				0.0%	0.0

Dynamic range (cont flux/line rms): N/A

Justification for requested RMS and resulting S/N (and for spectral lines the bandwidth selected) for the sensitivity ca...

Although we do not know for sure what the detailed surface brightness distribution will be for the targets in this sample, conservative simulations with smooth, power-law brightness distributions constrained by available low-resolution (~0.5" or better) data suggest that our inner disk surface brightness criterion (>20 mJy total inside a FWHM = 0.5" region) should provide >0.9 mJy per 50 mas beam inside a radius of ~0.25" (30 au). Note that the peak flux densities provided here could be significantly higher than this conservative lower bound. We are aiming for >5-sigma sensitivity to 10% brightness variations due to substructure in this region, which pushes us to the target RMS noise level of ~17 microJy per beam. Our direct experience with a large, similar dataset for Class II disks (from 2016.1.00484.L) confirms this criterion is sufficient for the stated goals.

Justification of the chosen angular resolution and largest angular scale for the source(s) in this Science Goal.

The angular resolution (range) we propose (25-50 mas) is designed to probe brightness features down to ~5 au (projected) spatial scales in the target disks, fine enough to resolve individual substructures like gaps carved by protoplanets or turbulent concentrations on scales comparable to the gas pressure scale height over most of the disk area. The acceptable range of resolution can be achieved with either the C43-8 or C43-9 configurations. While the maximum angular scale of these observations is quite small (0.3"), we have demonstrated in the comparably-designed Cycle 4 Large Program of Class II disks (2016.1.00484.L) that we can successfully recover all of the relevant flux and construct images with high fidelity by including compatible short spacings observations (see separate Science Goal). Again, the focus here is on appropriate measurements of the contrasts of substructure features in the inner disks, so resolving out larger scale envelope emission is not a problem (it is, in fact, desirable).

Justification of the correlator set-up with particular reference to the number of spectral resolution elements per line ...

These are pure TDM observations to maximize the bandwidth (1.875 GHz per SPW) and optimize sensitivity to continuum emission. The selection of Band 6 frequencies near 230 GHz provides the best balance of continuum sensitivity and allowable angular resolution in the standard modes.

Justification for non standard continuum frequencies.

The selected locations of the continuum spectral windows are designed to overlap with the short-spacings spectral line setup to optimally combine the datasets.

None Assigned

SG : 2 of 6 IRAS 04108+2803B long baselines Band 6

C43-8/9 observations to 17 uJy/beam.

Science Goal Parameters

Ang.Res.	LAS	Requested RMS	RMS Bandwidth	Rep.Freq.	Cont. RMS	Cont. Bandwidth	Poln.Prod.	Non-standard mode
0.0500" - 0.0250"	0.3"	17 µJy, 151.2 mK-604.8 mK	9588.245 km/s, 7.5 GHz	234.500000 GHz	16.946 µJy, 150.7 mK-602.9 mK	7.500 GHz	XX,YY	No

Use of 12m Array (43 antennas)

t_total(all configs)	t_science(C43-8,C4...	t_total()	Imaged area	#12m pointing	12m Mosaic spacing	HPBW	t_per_point	Data Vol	Avg. Data Rate
3.3 h	1.4 h	0.0 h	8.3 "	1	offset	24.8 "	4898.7 s	26.4 GB	3.3 MB/s

Use of ACA 7m Array (10 antennas) and TP Array

t_total(ACA)	t_total(7m)	t_total(TP)	Imaged area	#7m pointing	7m Mosaic spacing	HPBW	t_per_point	Data Vol	Avg. Data Rate

Spectral Setup : Single Continuum

Center Freq (Sky)	Center Freqs. SPWs	Eff #Ch p.p.	Bandwidth	Resolution	Vel. Bandwidth	Vel. Resolution	RMS
225.500000	216.500000	128	1875.00 MHz	31.250 MHz	2596.4 km/s	43.273 km/s	30.77 µJy, 1.3 K
	218.500000	128	1875.00 MHz	31.250 MHz	2572.6 km/s	42.876 km/s	30.86 µJy, 1.3 K
	232.500000	128	1875.00 MHz	31.250 MHz	2417.7 km/s	40.295 km/s	32.71 µJy, 1.2 K
	234.500000	128	1875.00 MHz	31.250 MHz	2397.1 km/s	39.951 km/s	34 µJy, 1.2 K

1 Target

No.	Target	Ra,Dec (ICRS)	V,def,frame --OR--z
1	1-IRAS_04108+2...	04:13:54, 28:11:32	4.00 km/s,lsrk,RADIO

Expected Source Properties

	Peak Flux	SNR	Linewidth	RMS (over 1/3 linewidth)	linewidth / bandwidth used for sensitivity	Pol.	Pol. SNR
Line	0.00 uJy	0.0	0 km/s			0.0%	0.0
Continuum	3.00 mJy	177.0				0.0%	0.0

Dynamic range (cont flux/line rms): N/A

Justification for requested RMS and resulting S/N (and for spectral lines the bandwidth selected) for the sensitivity ca...

Although we do not know for sure what the detailed surface brightness distribution will be for the targets in this sample, conservative simulations with smooth, power-law brightness distributions constrained by available low-resolution (~0.5" or better) data suggest that our inner disk surface brightness criterion (>20 mJy total inside a FWHM = 0.5" region) should provide >0.9 mJy per 50 mas beam inside a radius of ~0.25" (30 au). Note that the peak flux densities provided here could be significantly higher than this conservative lower bound. We are aiming for >5-sigma sensitivity to 10% brightness variations due to substructure in this region, which pushes us to the target RMS noise level of ~17 microJy per beam. Our direct experience with a large, similar dataset for Class II disks (from 2016.1.00484.L) confirms this criterion is sufficient for the stated goals.

Justification of the chosen angular resolution and largest angular scale for the source(s) in this Science Goal.

The angular resolution (range) we propose (25-50 mas) is designed to probe brightness features down to ~5 au (projected) spatial scales in the target disks, fine enough to resolve individual substructures like gaps carved by protoplanets or turbulent concentrations on scales comparable to the gas pressure scale height over most of the disk area. The acceptable range of resolution can be achieved with either the C43-8 or C43-9 configurations. While the maximum angular scale of these observations is quite small (0.3"), we have demonstrated in the comparably-designed Cycle 4 Large Program of Class II disks (2016.1.00484.L) that we can successfully recover all of the relevant flux and construct images with high fidelity by including compatible short spacings observations (see separate Science Goal). Again, the focus here is on appropriate measurements of the contrasts of substructure features in the inner disks, so resolving out larger scale envelope emission is not a problem (it is, in fact, desirable).

Justification of the correlator set-up with particular reference to the number of spectral resolution elements per line ...

These are pure TDM observations to maximize the bandwidth (1.875 GHz per SPW) and optimize sensitivity to continuum emission. The selection of Band 6 frequencies near 230 GHz provides the best balance of continuum sensitivity and allowable angular resolution in the standard modes.

Justification for non standard continuum frequencies.

The selected locations of the continuum spectral windows are designed to overlap with the short-spacings spectral line setup to optimally combine the datasets.

None Assigned

SG : 3 of 6 IRAS 04166+2706 long baselines Band 6

C43-8/9 observations to 17 uJy/beam.

Science Goal Parameters

Ang.Res.	LAS	Requested RMS	RMS Bandwidth	Rep.Freq.	Cont. RMS	Cont. Bandwidth	Poln.Prod.	Non-standard mode
0.0500" - 0.0250"	0.3"	17 µJy, 151.2 mK-604.8 mK	9588.245 km/s, 7.5 GHz	234.500000 GHz	16.968 µJy, 150.9 mK-603.6 mK	7.500 GHz	XX,YY	No

Use of 12m Array (43 antennas)

t_total(all configs)	t_science(C43-8,C4...	t_total()	Imaged area	#12m pointing	12m Mosaic spacing	HPBW	t_per_point	Data Vol	Avg. Data Rate
3.2 h	1.3 h	0.0 h	8.3 "	1	offset	24.8 "	4789.8 s	25.6 GB	3.3 MB/s

Use of ACA 7m Array (10 antennas) and TP Array

t_total(ACA)	t_total(7m)	t_total(TP)	Imaged area	#7m pointing	7m Mosaic spacing	HPBW	t_per_point	Data Vol	Avg. Data Rate

Spectral Setup : Single Continuum

Center Freq (Sky)	Center Freqs. SPWs	Eff #Ch p.p.	Bandwidth	Resolution	Vel. Bandwidth	Vel. Resolution	RMS
225.500000	216.500000	128	1875.00 MHz	31.250 MHz	2596.4 km/s	43.273 km/s	30.81 µJy, 1.3 K
	218.500000	128	1875.00 MHz	31.250 MHz	2572.6 km/s	42.876 km/s	30.9 µJy, 1.3 K
	232.500000	128	1875.00 MHz	31.250 MHz	2417.7 km/s	40.295 km/s	32.72 µJy, 1.2 K
	234.500000	128	1875.00 MHz	31.250 MHz	2397.1 km/s	39.951 km/s	34 µJy, 1.2 K

1 Target

No.	Target	Ra,Dec (ICRS)	V,def,frame --OR--z
1	1-IRAS_04166+2...	04:19:42, 27:13:38	4.00 km/s,lsrk,RADIO

Expected Source Properties

	Peak Flux	SNR	Linewidth	RMS (over 1/3 linewidth)	linewidth / bandwidth used for sensitivity	Pol.	Pol. SNR
Line	0.00 uJy	0.0	0 km/s			0.0%	0.0
Continuum	3.00 mJy	176.8				0.0%	0.0

Dynamic range (cont flux/line rms): N/A

Justification for requested RMS and resulting S/N (and for spectral lines the bandwidth selected) for the sensitivity ca...

Although we do not know for sure what the detailed surface brightness distribution will be for the targets in this sample, conservative simulations with smooth, power-law brightness distributions constrained by available low-resolution (~0.5" or better) data suggest that our inner disk surface brightness criterion (>20 mJy total inside a FWHM = 0.5" region) should provide >0.9 mJy per 50 mas beam inside a radius of ~0.25" (30 au). Note that the peak flux densities provided here could be significantly higher than this conservative lower bound. We are aiming for >5-sigma sensitivity to 10% brightness variations due to substructure in this region, which pushes us to the target RMS noise level of ~17 microJy per beam. Our direct experience with a large, similar dataset for Class II disks (from 2016.1.00484.L) confirms this criterion is sufficient for the stated goals.

Justification of the chosen angular resolution and largest angular scale for the source(s) in this Science Goal.

The angular resolution (range) we propose (25-50 mas) is designed to probe brightness features down to ~5 au (projected) spatial scales in the target disks, fine enough to resolve individual substructures like gaps carved by protoplanets or turbulent concentrations on scales comparable to the gas pressure scale height over most of the disk area. The acceptable range of resolution can be achieved with either the C43-8 or C43-9 configurations. While the maximum angular scale of these observations is quite small (0.3"), we have demonstrated in the comparably-designed Cycle 4 Large Program of Class II disks (2016.1.00484.L) that we can successfully recover all of the relevant flux and construct images with high fidelity by including compatible short spacings observations (see separate Science Goal). Again, the focus here is on appropriate measurements of the contrasts of substructure features in the inner disks, so resolving out larger scale envelope emission is not a problem (it is, in fact, desirable).

Justification of the correlator set-up with particular reference to the number of spectral resolution elements per line ...

These are pure TDM observations to maximize the bandwidth (1.875 GHz per SPW) and optimize sensitivity to continuum emission. The selection of Band 6 frequencies near 230 GHz provides the best balance of continuum sensitivity and allowable angular resolution in the standard modes.

Justification for non standard continuum frequencies.

The selected locations of the continuum spectral windows are designed to overlap with the short-spacings spectral line setup to optimally combine the datasets.

None Assigned

SG : 4 of 6 IRAS 04169+2702 long baselines Band 6

C43-8/9 observations to 17 uJy/beam.

Science Goal Parameters

Ang.Res.	LAS	Requested RMS	RMS Bandwidth	Rep.Freq.	Cont. RMS	Cont. Bandwidth	Poln.Prod.	Non-standard mode
0.0500" - 0.0250"	0.3"	17 µJy, 151.2 mK-604.8 mK	9588.245 km/s, 7.5 GHz	234.500000 GHz	16.957 µJy, 150.8 mK-603.3 mK	7.500 GHz	XX,YY	No

Use of 12m Array (43 antennas)

t_total(all configs)	t_science(C43-8,C4...	t_total()	Imaged area	#12m pointing	12m Mosaic spacing	HPBW	t_per_point	Data Vol	Avg. Data Rate
3.2 h	1.3 h	0.0 h	8.3 "	1	offset	24.8 "	4789.8 s	25.6 GB	3.3 MB/s

Use of ACA 7m Array (10 antennas) and TP Array

t_total(ACA)	t_total(7m)	t_total(TP)	Imaged area	#7m pointing	7m Mosaic spacing	HPBW	t_per_point	Data Vol	Avg. Data Rate

Spectral Setup : Single Continuum

Center Freq (Sky)	Center Freqs. SPWs	Eff #Ch p.p.	Bandwidth	Resolution	Vel. Bandwidth	Vel. Resolution	RMS
225.500000	216.500000	128	1875.00 MHz	31.250 MHz	2596.4 km/s	43.273 km/s	30.81 µJy, 1.3 K
	218.500000	128	1875.00 MHz	31.250 MHz	2572.6 km/s	42.876 km/s	30.9 µJy, 1.3 K
	232.500000	128	1875.00 MHz	31.250 MHz	2417.7 km/s	40.295 km/s	32.73 µJy, 1.2 K
	234.500000	128	1875.00 MHz	31.250 MHz	2397.1 km/s	39.951 km/s	34 µJy, 1.2 K

1 Target

No.	Target	Ra,Dec (ICRS)	V,def,frame --OR--z
1	1-IRAS_04169+2...	04:19:58, 27:09:57	4.00 km/s,lsrk,RADIO

Expected Source Properties

	Peak Flux	SNR	Linewidth	RMS (over 1/3 linewidth)	linewidth / bandwidth used for sensitivity	Pol.	Pol. SNR
Line	0.00 uJy	0.0	0 km/s			0.0%	0.0
Continuum	3.00 mJy	176.9				0.0%	0.0

Dynamic range (cont flux/line rms): N/A

Justification for requested RMS and resulting S/N (and for spectral lines the bandwidth selected) for the sensitivity ca...

Although we do not know for sure what the detailed surface brightness distribution will be for the targets in this sample, conservative simulations with smooth, power-law brightness distributions constrained by available low-resolution (~0.5" or better) data suggest that our inner disk surface brightness criterion (>20 mJy total inside a FWHM = 0.5" region) should provide >0.9 mJy per 50 mas beam inside a radius of ~0.25" (30 au). Note that the peak flux densities provided here could be significantly higher than this conservative lower bound. We are aiming for >5-sigma sensitivity to 10% brightness variations due to substructure in this region, which pushes us to the target RMS noise level of ~17 microJy per beam. Our direct experience with a large, similar dataset for Class II disks (from 2016.1.00484.L) confirms this criterion is sufficient for the stated goals.

Justification of the chosen angular resolution and largest angular scale for the source(s) in this Science Goal.

The angular resolution (range) we propose (25-50 mas) is designed to probe brightness features down to ~5 au (projected) spatial scales in the target disks, fine enough to resolve individual substructures like gaps carved by protoplanets or turbulent concentrations on scales comparable to the gas pressure scale height over most of the disk area. The acceptable range of resolution can be achieved with either the C43-8 or C43-9 configurations. While the maximum angular scale of these observations is quite small (0.3"), we have demonstrated in the comparably-designed Cycle 4 Large Program of Class II disks (2016.1.00484.L) that we can successfully recover all of the relevant flux and construct images with high fidelity by including compatible short spacings observations (see separate Science Goal). Again, the focus here is on appropriate measurements of the contrasts of substructure features in the inner disks, so resolving out larger scale envelope emission is not a problem (it is, in fact, desirable).

Justification of the correlator set-up with particular reference to the number of spectral resolution elements per line ...

These are pure TDM observations to maximize the bandwidth (1.875 GHz per SPW) and optimize sensitivity to continuum emission. The selection of Band 6 frequencies near 230 GHz provides the best balance of continuum sensitivity and allowable angular resolution in the standard modes.

Justification for non standard continuum frequencies.

The selected locations of the continuum spectral windows are designed to overlap with the short-spacings spectral line setup to optimally combine the datasets.

None Assigned

SG : 5 of 6 IRAS 04295+2251 long baselines Band 6

C43-8/9 observations to 17 uJy/beam.

Science Goal Parameters

Ang.Res.	LAS	Requested RMS	RMS Bandwidth	Rep.Freq.	Cont. RMS	Cont. Bandwidth	Poln.Prod.	Non-standard mode
0.0500" - 0.0250"	0.3"	17 µJy, 151.2 mK-604.8 mK	9588.245 km/s, 7.5 GHz	234.500000 GHz	16.975 µJy, 151 mK-603.9 mK	7.500 GHz	XX,YY	No

Use of 12m Array (43 antennas)

t_total(all configs)	t_science(C43-8,C4...	t_total()	Imaged area	#12m pointing	12m Mosaic spacing	HPBW	t_per_point	Data Vol	Avg. Data Rate
3.0 h	1.2 h	0.0 h	8.3 "	1	offset	24.8 "	4426.9 s	24.0 GB	3.3 MB/s

Use of ACA 7m Array (10 antennas) and TP Array

t_total(ACA)	t_total(7m)	t_total(TP)	Imaged area	#7m pointing	7m Mosaic spacing	HPBW	t_per_point	Data Vol	Avg. Data Rate

Spectral Setup : Single Continuum

Center Freq (Sky)	Center Freqs. SPWs	Eff #Ch p.p.	Bandwidth	Resolution	Vel. Bandwidth	Vel. Resolution	RMS
225.500000	216.500000	128	1875.00 MHz	31.250 MHz	2596.4 km/s	43.273 km/s	30.97 µJy, 1.3 K
	218.500000	128	1875.00 MHz	31.250 MHz	2572.6 km/s	42.876 km/s	31.05 µJy, 1.3 K
	232.500000	128	1875.00 MHz	31.250 MHz	2417.7 km/s	40.295 km/s	32.79 µJy, 1.2 K
	234.500000	128	1875.00 MHz	31.250 MHz	2397.1 km/s	39.951 km/s	34 µJy, 1.2 K

1 Target

No.	Target	Ra,Dec (ICRS)	V,def,frame --OR--z
1	1-IRAS_04295+2...	04:32:32, 22:57:26	4.00 km/s,lsrk,RADIO

Expected Source Properties

	Peak Flux	SNR	Linewidth	RMS (over 1/3 linewidth)	linewidth / bandwidth used for sensitivity	Pol.	Pol. SNR
Line	0.00 uJy	0.0	0 km/s			0.0%	0.0
Continuum	3.00 mJy	176.7				0.0%	0.0

Dynamic range (cont flux/line rms): N/A

Justification for requested RMS and resulting S/N (and for spectral lines the bandwidth selected) for the sensitivity ca...

Although we do not know for sure what the detailed surface brightness distribution will be for the targets in this sample, conservative simulations with smooth, power-law brightness distributions constrained by available low-resolution (~0.5" or better) data suggest that our inner disk surface brightness criterion (>20 mJy total inside a FWHM = 0.5" region) should provide >0.9 mJy per 50 mas beam inside a radius of ~0.25" (30 au). Note that the peak flux densities provided here could be significantly higher than this conservative lower bound. We are aiming for >5-sigma sensitivity to 10% brightness variations due to substructure in this region, which pushes us to the target RMS noise level of ~17 microJy per beam. Our direct experience with a large, similar dataset for Class II disks (from 2016.1.00484.L) confirms this criterion is sufficient for the stated goals.

Justification of the chosen angular resolution and largest angular scale for the source(s) in this Science Goal.

The angular resolution (range) we propose (25-50 mas) is designed to probe brightness features down to ~5 au (projected) spatial scales in the target disks, fine enough to resolve individual substructures like gaps carved by protoplanets or turbulent concentrations on scales comparable to the gas pressure scale height over most of the disk area. The acceptable range of resolution can be achieved with either the C43-8 or C43-9 configurations. While the maximum angular scale of these observations is quite small (0.3"), we have demonstrated in the comparably-designed Cycle 4 Large Program of Class II disks (2016.1.00484.L) that we can successfully recover all of the relevant flux and construct images with high fidelity by including compatible short spacings observations (see separate Science Goal). Again, the focus here is on appropriate measurements of the contrasts of substructure features in the inner disks, so resolving out larger scale envelope emission is not a problem (it is, in fact, desirable).

Justification of the correlator set-up with particular reference to the number of spectral resolution elements per line ...

These are pure TDM observations to maximize the bandwidth (1.875 GHz per SPW) and optimize sensitivity to continuum emission. The selection of Band 6 frequencies near 230 GHz provides the best balance of continuum sensitivity and allowable angular resolution in the standard modes.

Justification for non standard continuum frequencies.

The selected locations of the continuum spectral windows are designed to overlap with the short-spacings spectral line setup to optimally combine the datasets.

None Assigned

SG : 6 of 6 Short-Spacings Cluste Band 6

Observations at shorter spacings to improve self-calibration and imaging. All targets can be in a single cluster.

Science Goal Parameters

Ang.Res.	LAS	Requested RMS	RMS Bandwidth	Rep.Freq.	Cont. RMS	Cont. Bandwidth	Poln.Prod.	Non-standard mode
0.3000" - 0.1500"	1.7"	45 µJy, 11.1 mK-44.5 mK	7191.497 km/s, 5.6 GHz	234.500000 GHz	44.629 µJy, 11 mK-44.1 mK	5.625 GHz	XX,YY	No

Use of 12m Array (43 antennas)

t_total(all configs)	t_science(C43-5,C4...	t_total()	Imaged area	#12m pointing	12m Mosaic spacing	HPBW	t_per_point	Data Vol	Avg. Data Rate
2.1 h	1.2 h	0.0 h	8.3 "	5	offset	24.8 "	907.0 s	66.0 GB	10.6 MB/s

Use of ACA 7m Array (10 antennas) and TP Array

t_total(ACA)	t_total(7m)	t_total(TP)	Imaged area	#7m pointing	7m Mosaic spacing	HPBW	t_per_point	Data Vol	Avg. Data Rate

Spectral Setup : Spectral Line

BB	Center Freq Rest GHz	spw name	Eff #Ch p.p.	Bandwidth	Resolution	Vel. Bandwidth	Vel. Res.	Res. El. per FWHM
1	218.500000	continuum	128	1875.00 MHz	31.250 MHz	2572.7 km/s	42.878 km/s	0
2	219.980000	13CO + C18O	3840	937.50 MHz	0.564 MHz	1277.7 km/s	0.769 km/s	5
3	230.538000	CO v=0 2-1	3840	937.50 MHz	564.453 kHz	1219.2 km/s	0.734 km/s	5
4	234.000000	continuum	128	1875.00 MHz	31.250 MHz	2402.3 km/s	40.038 km/s	0

5 Targets

No.	Target	Ra,Dec (ICRS)	V,def,frame --OR--z
1	1-IRAS_04016+2...	04:04:43, 26:18:56	4.00 km/s,lsrk,RADIO
2	2-IRAS_04108+2...	04:13:54, 28:11:32	4.00 km/s,lsrk,RADIO
3	3-IRAS_04166+2...	04:19:42, 27:13:38	4.00 km/s,lsrk,RADIO
4	4-IRAS_04169+2...	04:19:58, 27:09:57	4.00 km/s,lsrk,RADIO
5	5-IRAS_04295+2...	04:32:32, 22:57:26	4.00 km/s,lsrk,RADIO

Expected Source Properties

	Peak Flux	SNR	Linewidth	RMS (over 1/3 linewidth)	linewidth / bandwidth used for sensitivity	Pol.	Pol. SNR
Line	30.00 mJy	9.2	4 km/s	3.28 mJy, 3.2 K	0.0006	0.0%	0.0
Continuum	20.00 mJy	448.1				0.0%	0.0

Dynamic range (cont flux/line rms): 21.4

1 Tuning

Tuning	Target	Rep. Freq. Sky GHz	RMS (Rep. Freq.)	RMS Achieved
1	1,2,3,4,5	234.496871	45.01 µJy, 44.5 mK	40.89 uJy - 48.59 uJy

Sensitivity Comments

Note that the bandwidth used for sensitivity is larger than 1/3 of the linewidth.
The S/N achieved for a resolution element that allows the line to be resolved will be lower than that reported.

Justification for requested RMS and resulting S/N (and for spectral lines the bandwidth selected) for the sensitivity ca...

Our experience with comparable observations of a large sample of Class II disks (2016.1.00484.L) confirm that we can optimize our image fidelity and recover emission on all of the relevant spatial scales by including measurements with a maximum angular scale ~2 arcseconds, provided they have high S/N. We are therefore targeting a continuum RMS noise level of 0.04
mJy/beam (aggregated over the full bandwidth), which should provide a peak S/N > 100 (our peak flux density estimates presume a flat intensity model for the brightness distribution based on ~0.5"-resolution previous observations) for all targets in this sample and would be sufficient to combine with the long-baseline observations and meet our science aims.

Justification of the chosen angular resolution and largest angular scale for the source(s) in this Science Goal.

These observations play a crucial support role to the primary focus of this proposal. Very long baselines are required to map small features in the targets, but the associated ALMA configurations lack the short spacings needed to recover the disk emission on all of the relevant spatial scales. We are targeting a maximum recoverable scale of 1.7 arcseconds, which is sufficient for all of the sample, given our knowledge of the source emission distributions from previous observations at ~0.5" angular resolution. This can be achieved with either the C43-5 or C43-6 configurations.

Correlator Comments

Note that the spectral resolution is larger than 1/3 of the the spectral line width and that your line may not be resolve

Justification of the correlator set-up with particular reference to the number of spectral resolution elements per line ...

The proposed correlator configuration strikes a balance between continuum bandwidth (for sensitivity and the main focus of the proposal) and spectral resolution that covers the 3 main CO(2-1) isotopologue lines (just over ~0.7 km/s resolution, sufficient for rotating disks). The expected line widths from the typical source in the sample is ~3-6 km/s, so we expect them all to be spectrally resolved. To optimize bandwidth, we have covered both the 13CO and C18O J=2-1 lines in the same 937.5 MHz spectral window: there is a safe border of >65 km/s in velocity width between these lines and the edges of the spectral window.

The sensitivity to these lines at the nominal resolution should be sufficient for standard assumptions (we estimate a peak S/N > 10 per channel on average in 12CO and 13CO, perhaps 3-5 for C18O), although realistically we do not know exactly what to expect when there is additional envelope emission.